Chapter 7

Structural Studies of BRCA1-KIF1b Complex

7.1 Introduction

Most of the intracellular trafficking occurs through the involvement of motor proteins such as kinesins. The kinesins belong to the super family of microtubule-stimulated ATPases, and are characterized by a conserved motor domain of ~350 amino acids. The Kinesin comprises different functional domains including microtubules interacting domain at C-terminal and adenine nucleotides interacting domain at N-terminal [204, 205]. Most kinesins ulitilize ATP-dependent motors to perform transport function of intracellular cargo using microtubules. These mechanochemical ATPases generate force to transport membrane bound vesicles, organelles or chromosomes towards the plus end of microtubules [206-209]. On the basis of sequence variability in the motor domain, kinesins can be classified into different families. Members of the same subfamily have highly conserved motor domains, particularly, at their extreme ends although the tail domain tends to be more different (**Figure 7.1**). The variable tail domain may specify the cargo molecule or organelle that is transported by a particular Kinesin Family member (KIF) [210]. KIF1 is one of the family and its most important member, KIF1B, was originally anticipated to be a motor for moving mitochondria toward microtubule positive end [211]. The *kif1b* gene was found to be located within a distal region of chromosome 1p, where loss of heterozygosity (LOH) is frequently observed in case of human neuroblastomas [212]. *kif1b* encodes as many as eight different isoforms that fall into two general classes of molecular weights: ~130,000 (KIF1Bp130) and ~204,000 (KIF1Bp204). The KIF1Bp130 class corresponds to the originally described KIF1B which binds to mitochondria through its unique C-terminal domain [213]. Mitochondria are the main cargo for KIF1b in addition to some other entities which remain to be

discovered [211]. Furthermore, a number of KIFs which are primarily found in neurons, are believed to participate in anterograde transport by carrying synaptic proteins and organelles from the neuronal soma [214]. Interactions with cargoes may also be regulated either by other kinesin-associated proteins or by phosphorylation of the polypeptide chain [215, 216]. The phosphorylation dependent interaction makes KIF1b a suitable candidate to study its role in DNA damage repair and cell -cycle regulation. It contains a pS-X-X-F motif which is commonly found in the BRCT domain interacting proteins.

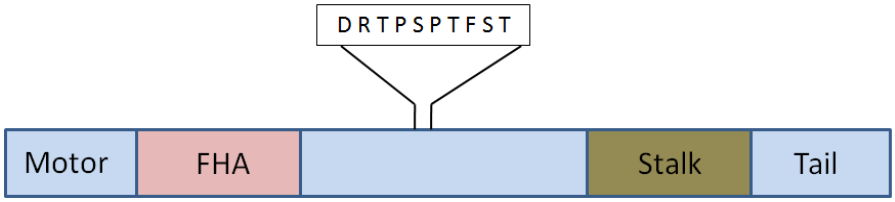

Figure 7.1: Schematic representation of the structure of KIF1b.

The BRCT domain is found in different proteins, including RAD9 [217], 53BP1[218], *Crb2* [219] and RAP1[220], and it possesses phosphopeptide-binding modules through which it functions in cell -cycle regulation , DNA-damage checkpoint control and DNA repair [10, 21]. Association of the sixth BRCT domain of TOPBP1 with E2F1 was shown to be regulated by phosphorylation [221]. BRCA1 BRCT phosphopeptide binding domains preferred aromatic amino acids at the position (+1) and hydrophobic or aromatic residues at the position (+2) [21]. However, towards the C-terminal to the phosphopeptide, phenylalanine at position (+3) is strongly preferred, hence this consensus sequences containing proteins are potential reported binding partners of the BRCA1 BRCT. This domain preferred a [YE]-E-[TV]-pS-[YFH]-[VTYF]-[FY] motif [21]. Different structures have already been reported in the Protein Data Bank in which BRCA1-BRCT showed its specificity towards (pS)-X-X-F motif containing protein such

as CTIP, BACH1[222, 223]. Moreover, other BRCT such as MDC1 BRCT also showed its specificity to the same consensus sequence [55]. Several structures of different BRCT domains in complex with phosphopeptide have been reported in the Protein Data Bank. For example, BRCA1 BRCT – BRCA1-Binding Helicase-Like Protein (BACH1; 1T29) complex structure, complex structure of BRCA1 BRCT and CtBP interacting protein (CtIP; 1Y98), structure of BRCA1 BRCT in complex with acetyl-CoA carboxylase 1 (ACC; 3COJ) and BRCT –tetrapeptide complex structure (3K0K) [91] [55] [224] [225]. Presence of similar domain in KIF1b prompted us to explore the binding mechanism with BRCT domain.

BRCA1 has two BRCT repeats at it C-terminal through which it regulates different functions such as DNA damage repair, cell cycle regulation, gene transcription and apoptosis [9, 63, 73, 226]. We were particularly intrigued by the possibility of BRCT domains mediating phosphorylation-dependent interactions, because protein phosphorylation by kinases is known to trigger the assembly of phosphorylation-dependent signaling pathways critical for cell growth and survival [227]. Different proteins that bind to phosphopeptides have been identified, including the BARD1, MDC1, XRCC1 [225, 227-230]. Each of these domains recognizes a subset of phosphorylated proteins which contain SPTF motif. From the synthetic peptide library search , it has been observed that KIF1b has pS-X-X-F containing motif [21]. An attempt was made to crystallize and determine the complex structure of BRCA1 BRCT domains in association with (pS)PTF containing phosphopeptide motif of KIF1b. A synthetic peptide having the sequence [NH2-DRTP(pS)PTFST-COOH] was used to determine the

binding affinity and mechanism of interaction between the KIF1b and BRCA1 BRCT (**Figure 7.2**).

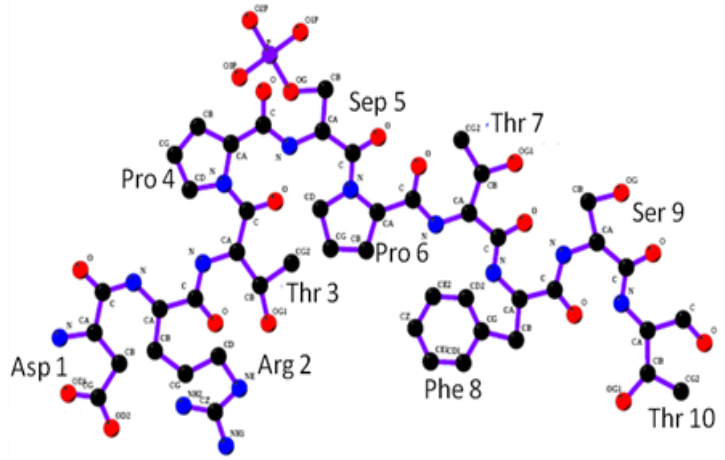

Figure 7.2: Schematic representation of Kif1b peptide used in the binding and structure determination study. SEP represents the phosphorylated serine.

7.2 Material and methods

7.2.1 Expression and Purification of BRCA1 BRCT domain: The pGEX-kT BRCA1 BRCT (1646-1859) construct was transformed into the bacterial expression host such as *E. coli* BL21 (DE3) strain, and the fusion protein was expressed using the methodology described in chapter 2. Expressed fusion protein was purified using GST affinity chromatography, and the GST tag was removed by treating the fusion protein with TEV protease. The purified protein was further subjected to size exclusion chromatography (AKTA- FPLC) Superdex- 200 column to get homogenous population. The purified BRCT domain was analysed by mass spectrometry to determine its exact molecular weight and identity.

7.2.2 Interaction analysis using ITC: The isothermal titration calorimetry reaction was performed by using *Microcal ITC 200* (GE, Sweden). The FPLC purified BRCA1 BRCT protein (0.02 mM) was titrated against the KIF1b phosphopeptide (0.200 mM). Both the protein and peptide were in same buffer containing 300 mM NaCl, 50 mM Tris, and pH-

7.5. BRCA1 BRCT protein was in sample cell while peptide solution from syringe was injected (2 µl each, total 16 injection) into the sample cell which was maintained at 25°C temperature by constant stirring at 1000 rpm (**Table 7.1**). The dissociation constant was calculated by fitting the sigmoidal curve using Origin software (Version 7.2). The heat of dilution was determined by titrating the peptide with the buffer and this was used for blank correction.

Table 7.1: ITC reaction parameters

Experimental parameters	
Total injections	16
Cell Temperature (°C)	25
Ref power (µcal/sec.)	5
Initial Delay (sec.)	250
Syringe conc. (mM)	0.2
Cell conc. (mM)	0.02
Stirring speed (RPM)	1000
Injection parameters	
Injection volume (µl)	2
Duration (sec.)	40
Spacing (sec.)	210
Pipette volume (µl)	~38
Filter period (sec.)	5

7.2.3 Protein crystallization: FPLC purified BRCA1 BRCT protein at a concentration of 25 mg/ml was used for setting crystallization trials as described in chapter 2. The concentrated protein was mixed with the synthetic KIF1b peptide (10 mg/ml) to obtain a 1:1.5 molar ratio concentration. This mixture was incubated overnight at 4°C and centrifuged before setting up for crystallization trial. Crystallization trials were set using commercially available crystallization kits (Hampton Research, Inc) using sitting and hanging drop methods. Initial crystallization drop volume of 2 µl containing 1 µl protein

and 1 µl mother liquor mixture was equilibrated through vapour diffusion against 0.5 ml of precipitant solution in the reservoir at 22°C. This crystallization conditions were observed at different time points, and further optimised by varying the concentration of precipitant and salt. The crystals were confirmed as protein crystals by staining with Izit dye from Hampton Research.

7.2.4 Diffraction data collection and processing: The BRCA1-KIF1b complex crystal was cryo-protected using 30% (v/v) glycerol as cryo-protectant prepared in mother liquor solution, and thereafter crystals were flash frozen in liquid

nitrogen before exposure to X-rays. Diffraction data were collected using rotating anode X-Ray Generator (Bruker) and Image plate (MAR Research), operated at 50 kV and 100 mA (Macromolecular X- diffraction facility at ACTREC). The crystal diffracted to about 3.5 Å resolution. A total of 237 oscillation frames were collected at 100 K with the detector set at a distance of 250 mm. The diffraction data were processed using iMOSFLM [231] software, and scaled using SCALA program from CCP4 suite [232]. V_M and filling map was calculated and solvent content was estimated [233].

7.2.5 Structure Solution of BRCT-KIF1b structure: Crystal structure of the BRCT-KIF1b complex was solved by Molecular Replacement (MR) using Phaser program [234]. The BRCA1 BRCT-CtIP complex structure (PDB ID-1Y98) was acquired from the Protein Data Bank, and was processed for removal of water and ligand molecules from the coordinate file, and was thereafter used as the search model [235]. The rotational and translation searches were carried out using PHASER software [236] and the MR solution was further refined by REFMAC 5 of CCP4 suite [232, 237]. Initially the model was refined as rigid body, and later rounds were of restrained refinement [237].

Table 7.2: Summary of data collection, processing and refinement statistics

Parameter	**Overall Value (highest resolution shell)**
No. of crystals used	1
X-ray source	Home source (ACTREC)
Wavelength (Å)	1.54179
Crystal to detector distance (mm)	250
Space group	$P2_12_12_1$
Unit cell parameters (Å)	a=84, b= 180.5, c=194 α=β= γ =90°
Vm ($Å^3$/Daltons) value	3.8
Total no. of residues	207
Mosaicity (°)	1.14
No. of molecule in asymmetric unit	8
Resolution limit (Å)	76.0-3.5 (3.69-3.50)
Total no. of reflections measured	218448
Unique reflections	32513
<Multiplicity>	6.7 (6.3)
$\langle I/\sigma(I) \rangle$	3.7 (1.1)
Completeness (%)	86
R_{merge} (%)	38.0 (147.7)
Refinement statistics	
R_{work} (%)	27.5
R_{free} (%)	31.8
Total no. of atoms used in refinment	14128
RMSD bond length (Å)	0.0089
RMSD bond angle (°)	1.3054
Ramachandaran plot	
Most favoured (%)	92.7
Additionally allowed (%)	6.1
Disallowed region (%)	0.8

A very tight Non Crystallography Symmetry (NCS) - restraints was imposed throughout the refinement (local NCS parameters: sigx 0.05, Maximum distance 4.2 Å, maximum difference of distances 1.0 Å). R_{free} was calculated as for R_{work} but only 5% data leftout of refinement procedure has been used in the calculations. In each cycle of refinement figure of merit (FOM), R_{free} and R_{work} was observed as the criterion for the selection of improved structure. Furthermore, electron densities of peptide and protein were monitored during each refinement to evaluate the improvement in the refined atomic model.

7.3 Results and discussion

7.3.1 Purification and Characterization of BRCA1 BRCT domain: The BRCA1 BRCT domain was successfully cloned into pGEX-kT vector and expressed in *E. coli* BL21 (DE3) strain. The protein, purified by affinity chromatography using GST sepharose 4B (Amersham) resins, showed a single band on SDS-PAGE (**Figure 7.3)**. On AKTA-FPLC, size exclusion column (Superdex -75), BRCA1 BRCT protein eluted at the expected elution volume and has shown the secondary peak corresponding to higher oligomer of BRCA1 BRCT. FPLC purified protein has shown a single band around 24 kDa on SDS PAGE (**Figure 7.3**). The mass profile showed a single peak which confirms homogeneity of the sample, and experimental molecular weight matched the expected value of 24660 Daltons.

7.3.2 Binding isotherm of BRCA1 BRCT domain and KIF1b peptide: The enthalpy change on interaction of BRCA1 BRCT with phosphopeptide of KIF1b was found to be sigmoidal in nature (**Figure 7.4)**. It has been observed that KIF1b phosphopeptide exothermically interacts with BRCA1 BRCT domain, and the binding affinity (K_d) of this

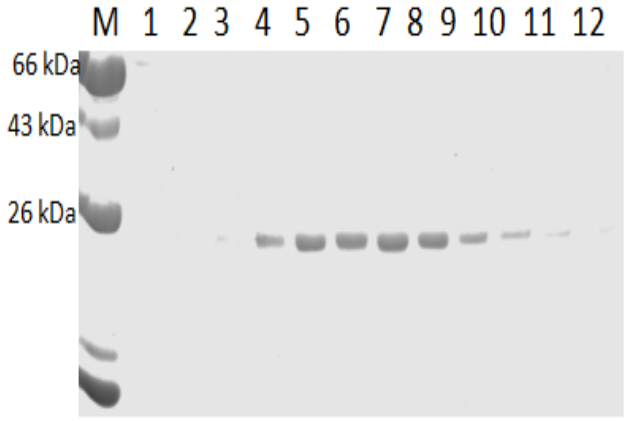

Figure 7.3: SDS-PAGE showing the FPLC purified protein BRCA1 BRCT

interaction was calculated to be 2.83 µM. So far the highest binding affinity is reported for BACH1 peptides having a K_d value of 0.9 µM. The weakest affinity is shown by the Acetyl CO-A peptide having a dissociation constant K_d 5.2 µM (**Table 7.3**). This suggests that KIF1b is one of the potential binding partner of BRCA1 BRCT.

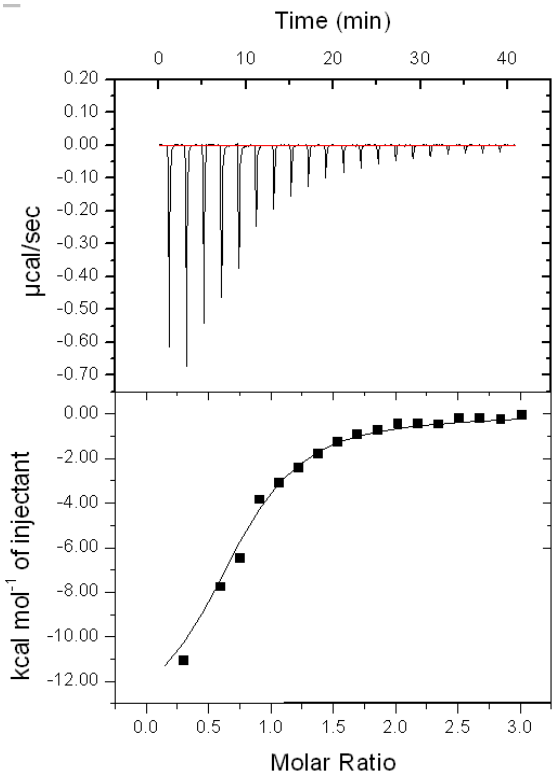

Figure 7.4: Binding isotherm of BRCA1 BRCT-KIF1b

Table 7.3: Binding comparison of various BRCA1 BRCT binding peptides

Complex	Peptide sequence	Dissociation constant (K_d)
BRCA1 BRCT-KIF1b	NH2-DRTP(pS)PTFST-COOH	2.83 µM
BRCA1 BRCT-ACC1	NH2-DSPPQ-pS-PTFPEAGH- COOH	5.2 µM
BRCA1 BRCT-BACH1	NH2-ISRSTpSPTFNKQ-COOH	0.9 µM
BRCA1 BRCT-CtIP	NH2-PTRVSpSPVFGAT-COOH	3.7 µM
BRCA1 BRCT-Tetrapeptide	NH2-pSPTF-COOH	3.7 µM

7.3.3 Crystallization and X-ray diffraction of BRCA1 BRCT domain: Crystals of the complex molecule were obtained by co-crystallization under following conditions: 0.2 M ammonium sulphate, 30% PEG 5000 MME, 0.1 M MES pH 7.5 using Hampton crystal screen. Purified protein produced hexagonal shape crystal during crystallization.

7.3.4 Structure solution of BRCA1 BRCT and KIF1b complex: Based on intensity equivalents, systematic absences and MR calculations, it has been observed that the crystal belongs to the space group $P2_12_12_1$ with unit cell parameters: a= 84.01 Å, b=180.47 Å , c=194.22 Å, α=β=γ=90°. The data processing statistics is given in **Table 7.2.** The useful data extend to 3.5 Å resolution, with a completeness of 86%. Calculated V_M value suggested presence of 8 molecules in the asymmetric unit. Molecular Replacement generated a single solution characterized by a TFZ score of around 10 and a log likelihood gain (LLG) score of about 105 [234]. The solution could be refined to obtain reasonably low value for crystallographic R-factor of 0.288 (**Table 7.2**). R_{free} value of 0.315 indicates good model fitting in the electron density at this resolution. The electron density map showed prominent electron density near Gly1656 and Ser1655

residue in the **F**o-**F**c difference map, confirming that the structure is of a molecular complex between BRCA1-BRCT and KIF1b peptide. Also, in the crystal structure, there is clear difference electron density for the KIF1b oligopeptides bound to all the eight subunits In the complex, eight of the ten residues of the ligand could be built successfully in the electron density map and refined satisfactorily. However, the terminal residue side chain showed weak electron density which may be due to disordered regions (**Figure 7.5**). The complete refinement statistics are given in **Table 7.2.** The major interactions between the KIF1b peptide and the BRCA1 BRCT domain are hydrogen bonds between phosphoserine 5 from the peptide and residues Ser1655 and Gly1656 from the BRCA1 BRCT domain (**Figure 7.5**). The nitrogen atom of Gly1656 and Oγ of Ser1655 form the hydrogen bonds with second oxygen of phosphate group of peptide Ser 5. Third oxygen of the phosphate group of peptide is involved in hydrogen bonding with side chain nitrogen atom of Lys1702. Similarly, carbonyl group of the Arg 1699 extend its hydrogen bonding through side chain carboxylic group of peptide Phe 8. The protein

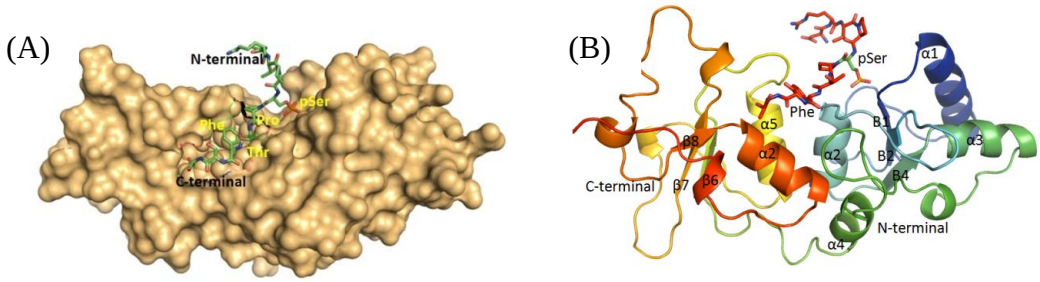

Figure 7.5: Structure solution of BRCA1 BRCT-KIF1b complex. (A) surface view of BRCT molecule along with KIF peptide. (B) Single chain BRCT with peptide.

peptide complex is stabilized by different hydrophobic interactions Val 1741, Met 1775, Phe 1704, Arg 1835 of protein with Phe 8 of peptide. There is also the hydrophobic

bonding contribution of Asn 1774 of protein with Pro 6 and Thr 7 of peptide (**Figure 7.6**) which indicate that the structure has been determined to good accuracy at this resolution.

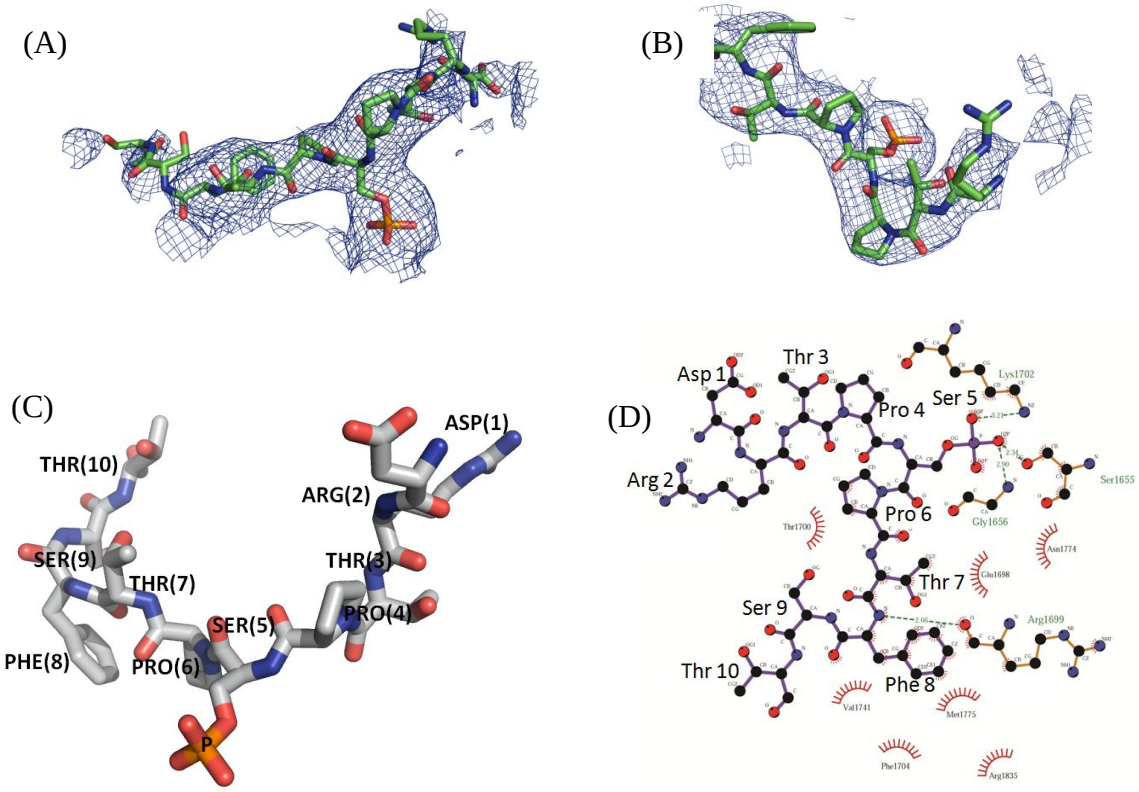

Figure 7.6: (A) and (B): Peptide showing electron density map (F_o-F_c, sigma cut off 1.0). (C) Stick representation of conformation of peptide. (D) Interaction analysis of BRCA1-BRCT with peptide KIF1b using LigPLOT. hydrogen bonds are shown as dashed lines, and hydrophobic interactions as arcs with radial spokes. This figure was made using LIGPLOT [238]

7.3.5 Structure analysis and validation: The overall quality and reliability of the structure was assessed with respect to energy and stereochemical geometry (overall quality factor (ERRAT): 93.86, Verify_3D (of 93.86% residues) score>0.2) [239]. The Ramachandran plot showed 99.0% of the residues were present in the allowed region [169] **(Figure 7.7)** [170, 171]. Verify_3D [239] profile revealed the average score 0.2 which is significant. Furthermore, structural geometry was evaluated using Mol Probity web server (http://molprobity.biochem.duke.edu/) which showed desired parameters in required range**.** There was no C_β deviation >0.25A° found in the structure. Similarly,

other structural pattern such as bad contact was around negligible. Values of some structural parameters are as follow, Wilson B-factor=64.3, Overall B-factor=47.47, Overall CC 1/2 value =0.966. Real space co-relation coefficient was 0.736463 for the peptide KIF1b. This indicates that the atomic parameters are in very good agreement with expected stereochemistry.

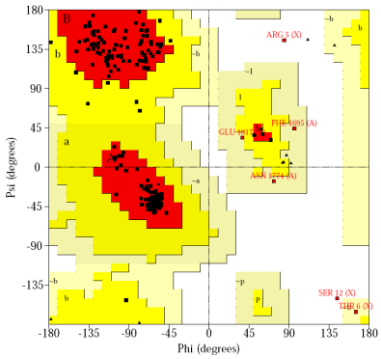

Figure 7.7: BRCA1 BRCT-KIF1b Ramachandaran plot (one monomer of asymmetric subunit)

7.3.6 Secondary and tertiary structure analysis of BRCA1 BRCT - KIF1b complex: The BRCA1 BRCT has two tandem repeats and consists of six α-helices and eight β- strands. The sequence of secondary structure followed in the BRCTs as β1-α1-β2-β3-α2-β4-α3-β5-α4-β6-α5-β7-β8-α6. Each BRCT is made up of three parallel β-strands and a single anti-parallel β-strand. The KIF1b peptide is present in the groove of BRCT domain, in which the phosphorylated Serine residue of KIF1b interacts with the N-terminal BRCT whereas C-terminal BRCT is involved in interaction with phenylalanine residue of the peptide (**Figure 7.8**).

7.3.7 Structural alignment of different chains of BRCA1 BRCT and peptide of asymmetric unit: There are eight molecules present in the asymmetric unit of BRCA1 BRCT-KIF1b complex structure. The average of the root mean square deviation (RMSD) between aligned structure of different chains of BRCTs present in the asymmetric unit is

0.09 Å (**Figure 7.9**) [240] over 203 Cα atom pairs, suggesting BRCT protein conformation remains same in different chains. Structural superposition of the eight of KIF1b ligands of asymmetric unit show greater variation (RMSD= 2.13 Å) towards its

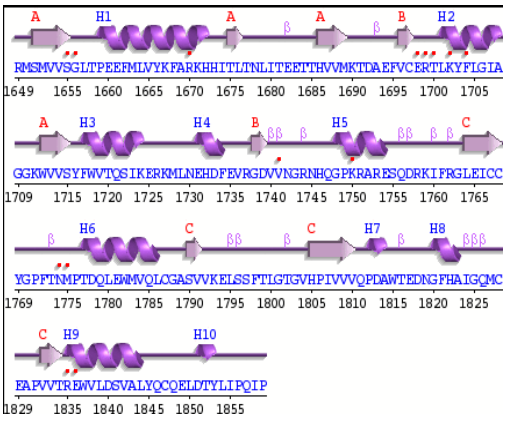

Figure 7.8: schematics representation of secondary structural component of BRCA1 BRCT-KIF1b.

terminal. However, the central tetrapeptide region, SPTF, superpose with the low RMSD of 0.274 Å (**Figure 7.9**) [31]. The peptide region which is involved in binding with the BRCT domain, particularly SPTF motif, thus maintains similar structural conformation.

7.3.8 Structural alignment of BRCA1 BRCT and KIF1b with reported structures:

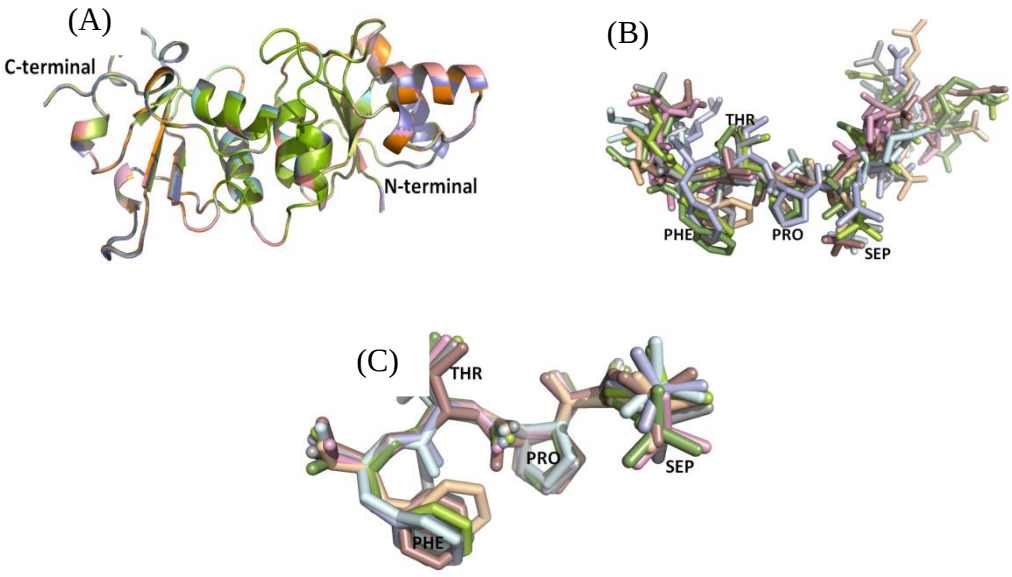

Figure 7.9: (A): Structural superposition of different chains of BRCA1-BRCT in asymmetric unit, without peptides. (B): Structural superposition of different chains of KIF1b in asymmetric unit, without BRCT. (C): Structural superposition of different chains of KIF1b (SPTF motif only) in asymmetric unit, without BRCT.

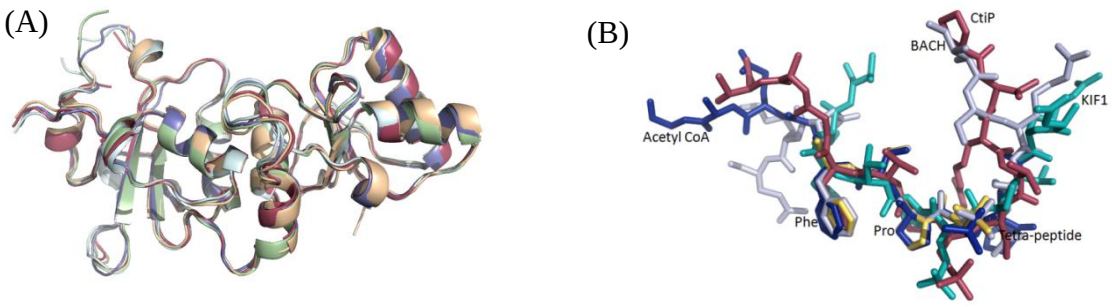

Figure 7.10: (A): Structural overlay of BRCA1-BRCT of the various reported complex with solve structure of BRCA1-BRCT, without peptides. Reddish brown, BRCA1 BRCT (PDB: 1JNX); Light Green, BRCT-BACH1 (PDB:1T29); Blue, BRCT-CtIP (PDB:1Y98); Golden, BRCT-ACOA (PDB: 3COJ), Light blue BRCT-tetrapeptide (PDB: 3K0K). (B): Structural overlay of reported BRCA1-BRCT bound peptides and KIF1b peptide

The RMSD between aligned structure of BRCA1 BRCT (PDB: 1JNX); BRCT-BACH1 (PDB:1T29); BRCT-CtIP (PDB:1Y98); BRCT-ACOA (PDB: 3COJ), BRCT-tetrapeptide (PDB: 3K0K) with solved structure showed a value of 0.34 Å (**Figure 7.10**) [240] over 203 Cα atom pairs, suggesting BRCT protein conformation largely remains unaltered upon ligand binding. Interestingly, central region of superpose peptides revealed a similar structural architecture towards the C-terminus of peptide and particularly between the residues proline and phenylalanine (**Figure 7.10**). The peptide region which is involved in binding with the BRCT domain remains structurally conserved, indicting a common mechanism of binding which might be critical for binding of phosphoserine specific ligands.

7.4 Conclusion

There are reports that numerous residues in the BRCA1 BRCT repeats are mutated in breast cancer cells [241, 242], However only reported pathogenic mutation could disrupt the interaction of BRCT domains with phosphorylated protein target thereby causing disease phenotypes. The KIF1b protein contains the signature sequence pS-X-X-F which is considered as a potential binding region for BRCA1-BRCT domain. There are

different BRCT domains containing proteins, MDC1[225], BARD1 [243], PARP1 [244] and XRCC1 [245], etc. which recognize phosphospecific binding partner [9]. BRCT domains, as phosphopeptide-interacting motifs, assist the congregation of proteins in complexes involved in signaling pathways that sense the activation of DNA damage and checkpoint kinases [9]. In the present studies, we found that KIF1b peptide binds to inter-BRCT domain with an affinity of 2.83 μM. The stoichiometry of binding to BRCT domain with peptides was found to be 1:1. The crystals of BRCT-KIF1b complex belong to the space group $P2_12_12_1$, and unit cell contains eight molecules per asymmetric unit. The complex structure of BRCA1 BRCT and KIF1b peptide was determined at 3.5 Å resolution. The pSer (0) and Phe (+3) in the bound peptide form the main centers of interaction with the BRCT domain. pSer interacts with N-terminal of BRCT through number of hydrogen bonds, while the Phe interacts with interface region and the C-terminal BRCT through hydrophobic interactions. pSer residue forms the hydrogen bond with Ser 1655 and Gly1656, and Phe is also involved in the hydrogen bonding with Arg1699, thereby stabilizing the complex. Phosphopeptide superposition reveals a common structural scaffold for the SPTF motif of peptide bound to the BRCT domain. Furthermore, pSer and Phe are the most common conserved residues involved in binding with BRCT. This provides a common mechanism of BRCT binding to its peptide and highlights the importance of mutations. The crystal structure of BRCA1 BRCT-KIF1b complex provides new insight into the molecular interactions of BRCA1 BRCT with various phospho-peptide and their binding specificities.